



Deposited via The University of York.

White Rose Research Online URL for this paper:

<https://eprints.whiterose.ac.uk/id/eprint/175114/>

Version: Published Version

Article:

Tang, Xinke, Kumar, Rupesh, Sun, Caiming et al. (2021) Towards underwater coherent optical wireless communications using a simplified detection scheme. *Optics Express*. pp. 19340-19351. ISSN: 1094-4087

<https://doi.org/10.1364/OE.426820>

Reuse



Items deposited in White Rose Research Online are protected by copyright, with all rights reserved unless indicated otherwise. They may be downloaded and/or printed for private study, or other acts as permitted by national copyright laws. The publisher or other rights holders may allow further reproduction and re-use of the full text version. This is indicated by the licence information on the White Rose Research Online record for the item.

Takedown

If you consider content in White Rose Research Online to be in breach of UK law, please notify us by emailing eprints@whiterose.ac.uk including the URL of the record and the reason for the withdrawal request.



Towards underwater coherent optical wireless communications using a simplified detection scheme

XINKE TANG,¹  RUPESH KUMAR,² CAIMING SUN,^{1,3,4,*}  LONG ZHANG,¹  ZHEN CHEN,¹ RUI JIANG,¹ HONGJIE WANG,³ AND AIDONG ZHANG^{1,3,4}

¹Robotics Research Center, Peng Cheng Laboratory (PCL), Shenzhen 518055, China

²Quantum Communications Hub and York Centre for Quantum Technologies, Department of Physics, University of York, YO10 5DD, UK

³Institute of Robotics and Intelligent Manufacturing (IRIM), The Chinese University of Hong Kong (CUHK), Shenzhen 518172, China

⁴Shenzhen Institute of Artificial Intelligence and Robotics for Society (AIRS), Shenzhen 518172, China
*cmsun@cuhk.edu.cn

Abstract: In this paper, an effective method of underwater coherent optical wireless communication (UCOWC) with a simplified detection scheme is proposed. The proof-of-concept experiments with M-ary PSK have been conducted with a common laser used for the signal source and local oscillator (LO). The BER performance has been evaluated at different underwater channel attenuations and the maximum achievable attenuation length (AL) with a BER below the forward error correction (FEC) limit of 3.8×10^{-3} is investigated. The tested system offers data rates of 500 Mbps, 1 Gbps, and 1.5 Gbps with the BPSK, QPSK and 8PSK modulated signals, respectively. The corresponding maximum achievable attenuation lengths are measured as 13.4 AL, 12.5 AL, and 10.7 AL. In addition, the performance degradation of the practical system with separate free running lasers for the signal and LO is also estimated. To the best of our knowledge, the UCOWC system is proposed and experimentally studied for the first time. This work provides a simple and effective approach to take advantages of coherent detection in underwater wireless optical communication, opening a promising path toward the development of practical UCOWC with next-generation underwater data transmission requirements on the capacity and transmission distance.

© 2021 Optical Society of America under the terms of the [OSA Open Access Publishing Agreement](#)

1. Introduction

Underwater wireless communication (UWC) plays a significant role in the underwater environment exploration, which has never been stopped and has gained a growing interest in recent years [1]. At present, the commonly used method for UWC is dominated by the acoustic communication, which offers long range communication in the water [2–4]. However, it suffers from the limited bandwidth and relative high latency, which makes it less favorable in the practical high-speed data transmission applications [1,5]. On the other hand, underwater optical wireless communication (UWOC) has attracted much attention in the recent years, which offers distinct advantages of high data rate up to Gbps, low latency, low power consumption, and small footprint [1]. UWOC has recently gained increasing research interest and significant progress on its performance has been achieved based on comprehensive study of transceiver design, modulation technique, as well as signal processing algorithms [6]. So far, nearly all UWOC experimental and practical systems are implemented based on the simplest method of intensity modulated direct detection (IM-DD). Although there have been a few promising UWOC demonstrations using phase shift keying (PSK) modulation or quadrature amplitude modulation (QAM) [7–9], they are actually

conducted by imposing intensity modulation on the pre-modulated signals and the signal is still directly detected [1]. In IM-DD systems, the desired information is carried only by the intensity of the sending light, and the data rate is limited by the system bandwidth affected by the intrinsic bandwidth of the transceiver [10]. Also, the practical performance of the IM-DD systems is seriously affected by the background and thermal noise at the receiver [11]. In contrast, the coherent approach (ie. coherent detection with enabled coherent modulation schemes) can be a promising solution. With a coherent receiver, full information can be restored on both In-phase (I) and Quadrature (Q) components of the complex amplitude of optical electric field [12–14]. It therefore can provide an additional degree of freedom available for encoding of information in UWOC and offer higher spectral efficiency compared to IM-DD systems [11,15]. For example, the multilevel phase shift keying (M-ary PSK) is one of the most commonly used modulation formats in the coherent communication systems, in which each symbol consists of $\log_2(M)$ bits and is encoded into a phase of a multiple of $2\pi/M$. The coherent receiver detects both IQ components and converts the optical carrier down to the baseband through the interference between the received signal and a strong reference light known as local oscillator (LO) [13]. Moreover, the other advantages of the use of coherent receiver over IM-DD systems are the higher receiver sensitivity due to the strong optical field of LO and better tolerance to background noise [11,16,17]. Despite these advantages, UWOC with coherent receiver has not been preferably investigated due to its higher implementation complexity than that with DD [5]. Indeed, the setup of a conventional coherent receiver requires two pairs of balanced detectors (BDs) as well as a 90-degree optical hybrid/mixer. Therefore, in order to take full advantages of coherent approach in underwater and make the coherent receiver an attractive prospect for the UWOC system, a simplified coherent detection scheme is proposed in this work. By using M-ary PSK modulation formats, the feasibility of the underwater coherent wireless optical communication (UCOWC) is experimentally demonstrated, which would open the door toward designing the next generation UWOC system with higher data rate and better sensitivity. The rest of the paper is organized as follows: Section 2 introduces the simplified receiver as well as the detection scheme. The feasibility of its application in UWOC is investigated via the proof-of-concept experiments and the experimental results are illustrated and discussed in Section 3. A brief conclusion of this paper is drawn in Section 4.

2. Simplified coherent detection scheme

The configuration of a typical coherent optical receiver is shown in Fig. 1 [13,18]. Please note that we consider only the single polarization of the signal here, while a polarization diversity configuration with twice the data rate can be realized by doubling the setup and adding two additional polarization beam splitters [13,18]. The complex optical field of the incoming signal (ie. received signal) has been modulated with the sending information at the transmitter side. In order to detect I and Q components, the received signal is branched into upper and lower paths to be mixed with the split LO separately [13,18]. The I component is obtained in the upper path and Q component is measured in the lower path with the phase of split LO rotated by 90 degrees. The optical circuit is known as the 90-degree optical hybrid. The resulting photocurrents at the output of the two balanced detectors can be expressed as [13,18]:

$$I_I(t) = R\sqrt{P_{sig}P_{LO}} \cos(\omega_{IF}t + \theta_{sig}(t) - \theta_{LO}(t)) \quad (1)$$

$$I_Q(t) = R\sqrt{P_{sig}P_{LO}} \sin(\omega_{IF}t + \theta_{sig}(t) - \theta_{LO}(t)) \quad (2)$$

where R is the photodiode's responsivity, P_{sig} and P_{LO} are the power of the signal laser and LO laser respectively, and ω_{IF} denotes the difference between the angular frequency of the LO and signal. In this paper, coherent receiver with homodyne detection is considered, therefore $\omega_{IF} = 0$. θ_{sig} and θ_{LO} are the phase of the signal laser and LO laser respectively.

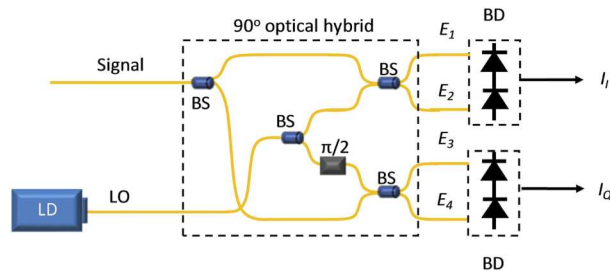


Fig. 1. Configuration of the coherent optical receiver, which contains a 90 degree hybrid mixer and two sets of balanced photodiodes (BD). LD: laser diode; LO: local oscillator; BS: beam splitter.

Based on the measurement of I_I and I_Q , the complex amplitude of the received optical signal can be recovered at the output of the receiver as $S = I_I + jI_Q$. Then, the symbols can be demodulated from the received signal and hence converted to the sending bits. As the mean square of the signal photocurrent in coherent detection is proportional to both P_s and P_{LO} , a gain in the output signal can be obtained. This leads to a higher detection sensitivity than direct detection [19]. In addition, the complex modulation formats can be introduced by using coherent detection, which provides a higher spectral efficiency [13]. However, these advantages come at the cost of higher implementation complexity. The conventional setup requires two BDs and a 90-degree optical hybrid consists of four couplers and a phase shifter. Such a detection scheme is less preferred in UWOC due to its higher optical complexity as well as the increasing insertion loss (introduced by the couplers).

In this work, we proposed a simplified coherent detection scheme as illustrates in Fig. 2(a). A single BD always detects only the projection on I axis of each pulse. In order to recover both In-phase and Quadrature values, each symbol/state (i, q) is represented by a two-pulse sample with an I pulse followed by a Q pulse. The first pulse (I pulse) represents the phase of the desired state (i, q) , thus the projection on I axis is $I_I = i$. The second pulse (Q pulse) represents the state with its phase rotated 90-degree clockwise so that its projection on I axis is equal to the Q information of

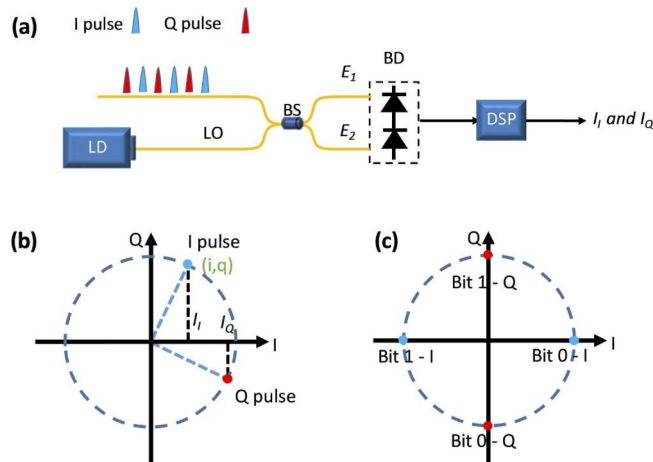


Fig. 2. (a) Configuration of the proposed detection scheme. (b) illustration of symbol encoding by a two-pulse sample. (c) example of BPSK coding diagram. LD: laser diode; DSP: digital signal processing

the desired state (ie. $I_Q=q$). The photocurrent can be mathematically expressed as:

$$I \text{ pulse} : I(t) = R\sqrt{P_{sig}P_{LO}} \cos(\omega_{IF}t + \theta_{sig}(t) - \theta_{Lo}(t)) \quad (3)$$

$$Q \text{ pulse} : I(t) = R\sqrt{P_{sig}P_{LO}} \cos \left[\omega_{IF}t + \left(\theta_{sig}(t) - \frac{\pi}{2} \right) - \theta_{Lo}(t) \right] \quad (4)$$

As a result, the coherent detection can be realized and full information of the received signal can be recovered. For example, in a BPSK format, bit 0 is encoded into a 0-degree constellation point followed by a 270-degree constellation point, while bit 1 is encoded into a 180-degree constellation point followed by a 90-degree constellation point, as shown in Fig. 2(c). This proposed setup more than halves the optical complexity and the insertion loss, and also simplifies the calibration procedure. Although the spectral efficiency is halved due to the 50% redundancy in the data stream, it can be compensated by the deployment of multilevel modulation schemes. The spectral efficiency and the overall data rate can be further improved with the increased number of modulation levels.

3. Application in UWOC

3.1. Proof-of-concept experiments

The proposed detection scheme enables the realization of underwater coherent optical wireless communication. With the proposed detection scheme, coherent modulation can be conducted in the transmitting site, and the receiver can identify I and Q components (ie. both of the quadratures) with improved sensitivity. The experimental setup is illustrated in Fig. 3(a). A continuous wave laser (center wavelength of 532 nm and a linewidth $\Delta\nu < 1$ MHz) is modulated by an external optical phase modulator based on the encoded signal from an arbitrary waveform generator (AWG), as discussed in Section 2. The symbol rate is operated at 1 GS/s with BPSK, QPSK and 8PSK modulation formats. The power from the transmitter is fixed at 10 dBm (10mW). The modulated optical signal is then sent to the water channel via a fiber collimator as parallel wireless beam. The water channel is simulated by a glass water tank (1 m \times 0.4 m \times 0.25 m) filled with tap water, of which the attenuation coefficient is measured as about $c=0.3 \text{ m}^{-1}$. The underwater transmission distance is extended to 10 meters (1 meter \times 10) by placing two highly reflective mirrors at both ends of the water tank. Figure 3(b) shows the reflected path of the laser beam in the water tank. The photo is taken in the dark in order to clearly observe the laser trace, while our experiments are conducted in a normal indoor lighting condition (ambient light at the optical table is about 30 μ W). The channel attenuation and hence the received optical power is varied by adding Maalox ($Al(OH)_3$ and $Mg(OH)_2$) solution, which has been widely used for varying the turbidity of water [1,20,21]. A polarization controller (PC) is employed to match the polarization of the signal to that of LO and the LO power is fixed at 4 mW at the input of the receiver. The received signal is demodulated by the proposed coherent detection with a 1 GHz balanced detector. The detected signal is then captured by a 20 GS/s software controlled oscilloscope (Keysight DSOS254A). The bit error rates (BERs) calculation are conducted in an offline Matlab program after the data transferred from the oscilloscope to a computer. Specifically, the captured signal is decoded back into symbols with a searched optimum decision threshold after the synchronization, and the bits belonging to each symbol are Gray coded in order to minimize the bit error rate [13]. The alignment between the received and transmitted signal is conducted via the use of cross-correlation. The BER is then calculated by the comparison between the decoded bits and the transmitted bits. In this work, M-ary PSK modulation is employed to demonstrate the feasibility of proposed detection scheme and its application in the coherent UWOC system by the use of phase modulator (PM) and a continuous wave (CW) laser. A single laser is used in this feasibility study for both the transmitter and the receiver setup due to the limited resources. The LO is indicated by the dotted line in Fig. 3(a). In

practical UCOWC implementations, two tunable laser sources are required for the signal and LO separately. The matching of the emission wavelength of signal and LO lasers can be realized by bias current and temperature tuning. If the laser requires further minimization of the frequency drift, an additional step of carrier frequency estimation and recovery could be added, which can be practically compensated by the mature means of digital signal processing [22–24]. However, the linewidths of the signal and LO lasers would inevitably cause additional phase noise, and the possible influence of this in our experimental results would be discussed in Section 3.2.

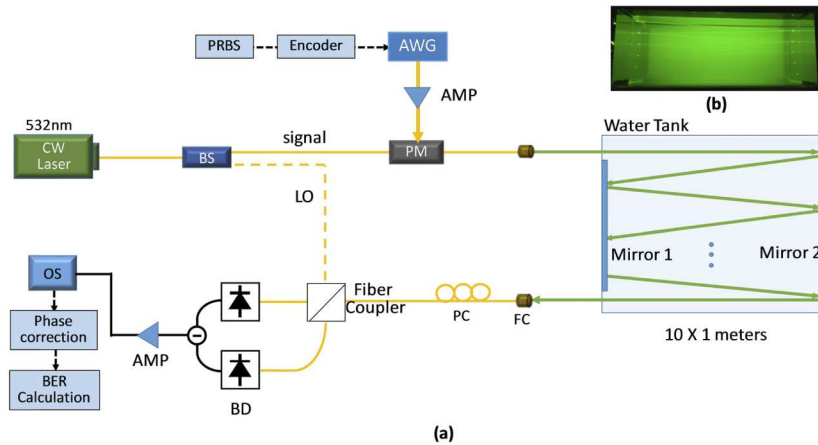


Fig. 3. (a) Schematic of experimental setup for a proof-of-concept demonstration of UCOWC. (b) The reflected paths of the laser beam in the water tank. BS: beam splitter; FC: fiber collimator; AMP: RF amplifier; PRBS: pseudo random bit sequence; OS: oscilloscope

In addition, the finite linewidth of the laser and the different optical paths from the signal and the LO to the coherent receiver would cause random rotation in the phase of signal relative to phase reference of the LO. Fortunately, the phase rotates much slower than the symbol rate. Therefore, in order to deploy the proposed receiver in UWOC system, we estimate and correct the random phase rotation by sending pilot pulses as a header in each signal pulse data block. Inspired by the work in [25], the pilot pulses in each data block are initially set to have three different phase rotations in the transmitting signal (0° , 120° , and 240°), as shown in Fig. 4.

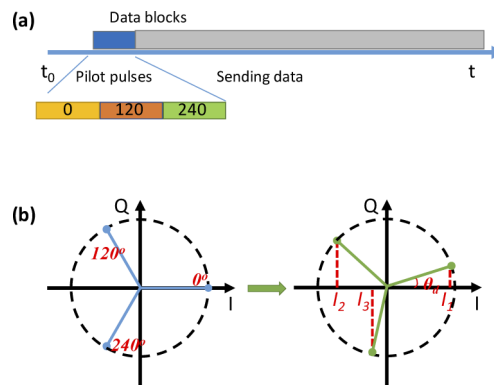


Fig. 4. Illustration of (a) the data block (b) the phase drift in pilot pulses

When the signal arrives at receiver, the phase of each data block is drifted and rotated by an arbitrary angle of θ_d with respect to the phase of the LO pulses. By using the measurement of

the average I value of those three sets of pilot pulses, namely I_1 , I_2 , and I_3 , this angle can be estimated as:

$$\theta_d = -\tan^{-1} \left[\frac{\sqrt{3}(I_3 - I_2)}{2I_1 - I_2 - I_3} \right] \quad (5)$$

After estimating θ_d , the received phase value can be accordingly corrected by the use of rotation matrix:

$$\begin{bmatrix} I' \\ Q' \end{bmatrix} = \begin{bmatrix} \cos(\theta_d) & \sin(\theta_d) \\ -\sin(\theta_d) & \cos(\theta_d) \end{bmatrix} \begin{bmatrix} I \\ Q \end{bmatrix} \quad (6)$$

Where I and Q are measured values, I' and Q' are corrected values. They are then used for bit error rate calculation by comparing them with the transmitting I/Q pairs.

3.2. Results and discussion

The system performance of this UCOWC lab demonstration with the proposed simplified coherent detection is investigated. With the setup introduced in the previous section, the proposed detection scheme including the phase correction method is experimentally verified. As an example, the constellation diagrams of the received signal at power of about -40 dBm are shown in Fig. 5 (with and without phase correction). The experimental measurements are conducted via block by block data transfer from an oscilloscope to a computer, and each constellation diagram corresponds to a collection of 2^{14} samples. Firstly, it can be seen from Fig. 5 that the I and Q components of the received signal are successful identified from interleaved I and Q pulses as illustrated in Fig. 2. Secondly, θ_d can be estimated and corrected for the data within a block by the method illustrated in Fig. 4. As shown in the constellation diagrams for BPSK QPSK and 8PSK modulated signals without phase correction, θ_d are about 65, 186 and 71 degrees in the collected data blocks respectively, and the constellation diagrams can be corrected into the right position with the phase correction method as shown in bottom plots in Fig. 5.

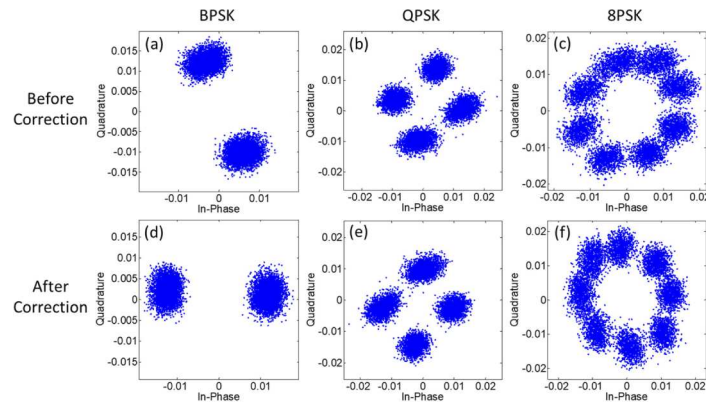


Fig. 5. Constellation diagrams of the received BPSK, QPSK and 8PSK signals (a)-(c) before phase correction and (d)-(f) after phase correction, respectively.

The experimental results are shown in Fig. 6. The symbol error rates (SERs) of the proposed UCOWC system are calculated by comparing the received symbols with the transmitted symbols, which are then plotted in Fig. 6(a) as a function of received power for BPSK, QPSK and 8PSK signals. The bit error rates are obtained after the conversion from symbols to bits, which are shown in Fig. 6(b). It can be seen that both the SER and BER increase with the water channel attenuation as well as the number of modulation levels. The forward error correction

(FEC) threshold of 3.8×10^{-3} [2], which is the maximum BER level which a standard FEC code can operate, is plotted as a green dashed line in Fig. 6(b). The constellation diagrams of the received BPSK, QPSK and 8PSK signals around FEC limit are plotted in Fig. 6(c), (d) and (e), respectively. It can be seen from the experimental results, in order to achieve a feasible UCOWC transmission with BERs below the FEC threshold, the minimum required received powers (ie. the sensitivity of the receiver) are about -48.2 dBm, -44.1 dBm and -36.6 dBm for BPSK, QPSK and 8PSK respectively. The corresponding ratios of P_{LO} to P_{sig} are 54.2 dB, 50.1 dB and 42.6 dB, respectively.

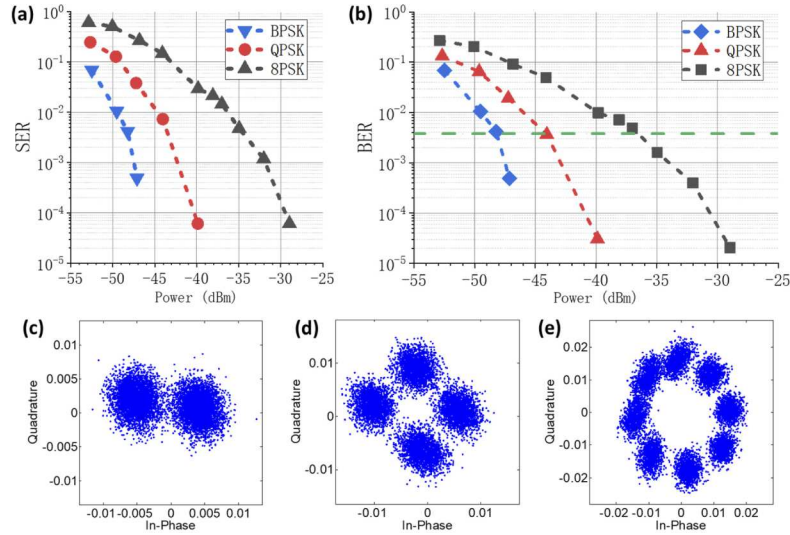


Fig. 6. (a) SERs as a function of received power for demodulation of BPSK, QPSK and 8PSK signals (b) BERs as a function of received power for demodulation of BPSK, QPSK and 8PSK signals (c)-(e) Constellation diagrams of the received BPSK, QPSK and 8PSK signals near the FEC limit.

As mentioned in the previous section, the proposed detection scheme significantly reduces the implementation complexity of a coherent receiver for UWOC system, but at a cost of a 50% redundancy in the data train. Fortunately, the reduced data rate in a UCOWC system can be compensated or even increased by higher level modulation formats which are consequently enabled by the use of coherent receiver. Given that the system repetition rate is fixed at 1 GHz in this feasibility study, BPSK, QPSK, and 8PSK offers a data rate of 500 Mbps, 1 Gbps, and 1.5 Gbps respectively. Please note that the experiments have been conducted in a normal indoor lighting condition, and we have tested that the proposed system is rarely affected by ambient light.

As mentioned above, only one common laser is used for signal and LO in the proof-of-concept experiments due to the limited resources. The feasibility of the proposed coherent detection scheme in UWOC has been demonstrated with a common laser, and the system can be also implemented with two lasers in practical applications. However, the extra phase noise introduced by the separate free-running laser has to be considered. Specifically, having two lasers centered around the same wavelength and with linewidths $\Delta\nu_1$ and $\Delta\nu_2$, the relative phase variance can be modeled as a function of system symbol rate R_s [26–28]:

$$Var_{phase} = 2\pi \frac{\Delta\nu_1 + \Delta\nu_2}{R_s} \quad (7)$$

Thus, we can estimate the system performance of the practical case with separate lasers for signal and LO generation by adding this noise term into the experimentally measured data [13]:

$$I_{out}(t) = I_I(t) + iI_Q(t) = R\sqrt{P_{sig}P_{LO}} \exp(i\theta_s) \exp(i\theta_n) \quad (8)$$

where I_{out} is the complex amplitude output from the receiver, θ_s is the phase modulation, and θ_n is the additional phase noise.

The updated results in terms of the sensitivity with the simulated additional phase noise with different combined linewidth values are plotted in Fig. 7. The practical case with two free-running lasers would cause an additional contribution to the phase noise, and the increase of the sum of linewidth leads to an increase in BER and hence the degradation in the sensitivity of the receiver. In addition, it can be seen that such a degradation is more noticeable for the higher level modulation format. BPSK offers better laser linewidth tolerance, due to the wider separation between signal states on the constellation diagram.

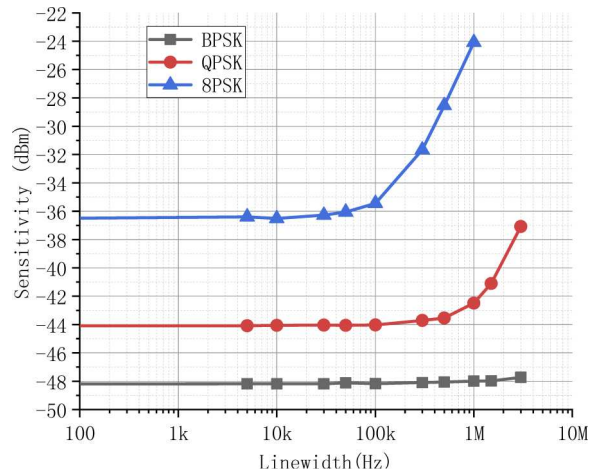


Fig. 7. The sensitivity for detecting BPSK, QPSK and 8PSK signals at the BER= 3.8×10^{-3} as the function of the sum of the linewidths of the signal and local oscillator lasers.

On the other hand, as mentioned in Section 2, coherent receiver offers effective amplification on the received signal by the use of LO. Therefore, proposed system also provides the efficient gateway towards to long-distance underwater data transmission. As the underwater transmission distance also affected by the water types, Attenuation Length (AL) is the commonly used distance unit in the evaluation of the UWOC systems [29]. It is the product of the attenuation coefficient of water c , and the transmission path length L , and can be also expressed as a function of the path loss in dB (Loss) [29]:

$$AL = c \times L = -\ln(10^{-Loss/10}) \quad (9)$$

The achievable AL is in fact affected by the transmitting power and the sensitivity of the detection system. In order to evaluate the tested system in this work, we calculated the achievable AL given that the transmitted power is fixed at 10dBm in the experiments. The results are summarized in Table 1. It can be seen that the calculated maximum achievable AL for BPSK QPSK and 8PSK (with a data rate of 500 Mbps, 1 Gbps and 1.5 Gbps, respectively) are around 13.4, 12.5 and 10.7 for the common laser case. On the other hand, in a practical case with combined linewidth of 1 MHz, the sensitivity of the detection system is decreased to -47.9 dBm, -42.5 dBm and -24.1 dBm and hence the achievable AL would be 13.3, 12.1 and 7.9.

Table 2 shows representative configurations and performances of recent IM-DD UWOC systems. The AL is extended straightforwardly by the employment of higher sensitive detector

Table 1. The sensitivities and achievable ALs

System Speed	BPSK (500Mbps)	QPSK (1Gbps)	8PSK (1.5Gbps)
Sensitivity (common laser)	-48.2dBm	-44.1dBm	-36.6 dBm
Achievable AL (common laser)	13.4	12.5	10.7
Sensitivity (separate lasers)	-47.9dBm	-42.5dBm	-24.1dBm
Achievable AL (separate lasers)	13.3	12.1	7.9

and/or higher power laser. Typically, the maximum AL achieved in IM-DD systems at Gbps data rate is less than 7 AL [30–35]. Recently, we have demonstrated a 11.6 AL/1 Gbps UWOC using a highly sensitive silicon photomultiplier (SiPM) based receiver [29]. To the best of authors' knowledge, that is the largest AL achieved in reported IM-DD UWOC systems with a data rate above 1 Gbps. However, the performance from [29] was achieved in the dark and the receiver was covered in a black box (ambient light is about 1 nW), as the SiPM is very sensitive to the ambient light. In this paper, the proposed coherent system with PIN balanced detector provides much better background noise rejection. On the other hand, a long-reach IM-DD system with highly sensitive multi-pixel photon counter (MPPC) based receiver has been recently demonstrated with three 1W high power lasers (total output power is 2.4 W), but the data rate is only about 8.4 Mbps and 16.8 Mbps at AL of 24 and 12 [36]. In this paper, the proposed method provides a promising path toward taking advantages of coherent detection in UWOC, which opens the possibility for higher data rate, better sensitivity as well as better tolerance to background noise. With the detection scheme demonstrated in this paper, the data rate is possible to be further increased by the deployment of more advanced modulation formats with increased spectral efficiency and degree of flexibility, such as 16-QAM and 32-QAM, and the achievable AL can be extended by having higher LO power. That would require the replacement of the phase modulator with an integrated I/Q electro-optic modulator and higher power LO laser, which is beyond the scope of this feasibility study but can be part of our future investigations.

Table 2. IM-DD UWOC system's performance

Paper	Photodiode	Modulation	Tx Optical Power	AL	Data Rate
[30]	APD	OOK	51.3 mW (LD)	1.7	1.5 Gbps
[31]	APD	OOK	19.4 mW (LD)	3.495	2.7 Gbps
[32]	APD	OFDM	45 mW (LD)	2.35	4 Gbps
[33]	APD	DFT-S DMT	16.18 mW (LD)	<5.5	5 Gbps
[2]	APD	OOK	7.25 mW (LD)	5.162	500 Mbps
[34]	APD	OOK	50.2 mW (LD)	4.27	2.5 Gbps
[35]	APD	OOK	10 mW (LD)	6.682	1.9 Gbps
[29]	SiPM	OOK	10 mW (LD)	11.6	1 Gbps
[36]	MPPC	NRZ-OOK	2.4 W (3×LD)	24	8.4 Mbps
				12	16.8 Mbps

Similar to other UWOC systems, scattered photons may travel multiple paths in the water channel toward to the coherent receiver. As the multipath components with different phase and amplitude reach to the receiver at different time instants, the received scattered photons from the previous symbols will interfere with the subsequent symbols. This would cause the inter-symbol interference (ISI) in the detected signal [37]. The multipath effect is getting enhanced with the increased scattering events, but can be neglected when too few scattered photons are received. In this work, the ISI was not observed and can be neglected in our proof-of-concept experiments,

but has to be considered for the case with more turbid water and longer transmission distance [1]. The detailed study related to the scattering effect based on Monto Carlo method can be found in [37].

Moreover, it is interesting to note that the above lab demonstration with the proposed detection scheme also validates the practical UCOWC implementation in a retro-reflective (RR) link configuration with a common laser source. Both the light source and the receiver are located at one side of the system. Such a configuration has been proposed for the UWOC system with restricted weight and power budget, such as an underwater sensor node [1]. The continuous wave beam is sent out from one end and modulated and reflected back by a modulating retroreflector at the other end [1]. Thus, the information is encoded on the reflected light and detected by the receiver placed at the same end with the laser source. However, the application of conventional RR UWOC systems is limited by the short transmission distance as optical signals from the receiving site are propagating the underwater channel twice. Therefore, it can be predicted that the application of proposed coherent receiver is able to increase the sensitivity hence to compensate the enhanced channel attenuation, while the employment of RR link configuration can eliminate the requirement of two laser sources in the practical UCOWC with direct link configuration.

4. Conclusion

In this work, a simplified coherent receiver with homodyne detection is proposed with effective coding method of using redundancy in data transmission. This leads to significant simplification in the design and implementation compared with the conventional coherent receiver, which enhances the potential of using the coherent method in UWOC systems. The feasibility of the proposed receiver in a UWOC system is experimentally demonstrated, using a common laser source for the signal and LO. It offers a data rate of 500 Mbps, 1 Gbps, and 1.5 Gbps with the BPSK, QPSK and 8PSK modulated signals, and the corresponding AL is measured as 13.4 AL, 12.5 AL, and 10.7 AL. We also estimated the impaired performance in a practical case with two separate lasers. For a combined linewidth of 1 MHz, and the maximum achievable AL is degraded to 13.3 AL, 12.1 AL, and 7.9 AL for BPSK, QPSK and 8PSK respectively.

To the best of our knowledge, the UCOWC system is proposed and experimentally studied for the first time, which offers a promising path toward the underwater data transmission with higher data rate and better sensitivity. Our future investigations will include conduction of a fully operational practical UCOWC system with two separate lasers in the transmitter and receiver sites, as well as the study of more advanced modulation formats. The promising method demonstrated in this paper can be even used in underwater quantum coherent communications.

Funding. Collaborative Operation Platform for Smart Underwater Robots (COPSUR) through the PCL Key Project; Shenzhen Natural Science Foundation (JCYJ20180508163015880); National Natural Science Foundation of China (U1813207, U1613223); Guangdong Science and Technology Innovation Foundation (2019TQ05X062).

Acknowledgments. R. K. thanks the support from EPSRC Quantum Communications Hub (Grant No. EP/T001011/1).

Disclosures. The authors declare that there are no conflicts of interest related to this article.

Data availability. Data underlying the results presented in this paper are not publicly available at this time but may be obtained from the authors upon reasonable request.

References

1. Z. Zeng, S. Fu, H. Zhang, Y. Dong, and J. Cheng, "A Survey of Underwater Optical Wireless Communications," *IEEE Commun. Surv. Tutorials* **19**(1), 204–238 (2017).
2. J. Wang, C. Lu, S. Li, and Z. Xu, "100 m/500 Mbps underwater optical wireless communication using an NRZ-OOK modulated 520 nm laser diode," *Opt. Express* **27**(9), 12171–12181 (2019).
3. H. M. Oubei, C. Shen, A. Kammoun, E. Zedini, K.-H. Park, X. Sun, G. Liu, C. H. Kang, T. K. Ng, M.-S. Alouini, and B. S. Ooi, "Light based underwater wireless communications," *Jpn. J. Appl. Phys.* **57**(8S2), 08PA06 (2018).
4. N. Saeed, A. Celik, T. Y. Al-Naffouri, and M.-S. Alouini, "Underwater optical wireless communications, networking, and localization: A survey," *Ad. Hoc. Networks* **94**, 101935 (2019).

5. H. Kaushal and G. Kaddoum, "Underwater Optical Wireless Communication," *IEEE Access* **4**, 1518–1547 (2016).
6. J. Xu, "Underwater wireless optical communication: why, what, and how? [Invited]," *Chin. Opt. Lett.* **17**(10), 100007 (2019).
7. B. Cochenour, L. Mullen, and A. Laux, "Phase Coherent Digital Communications for Wireless Optical Links in Turbid Underwater Environments," *OCEANS 2007*, Vancouver, BC, Canada, 1–5 (2007).
8. A. Al-Halafi, H. M. Oubei, B. S. Ooi, and B. Shihada, "Real-time video transmission over different underwater wireless optical channels using a directly modulated 520 nm laser diode," *J. Opt. Commun. Netw.* **9**(10), 826–832 (2017).
9. M. C. Gökçe, Y. Baykal, and Y. Ata, "M-ary phase shift keying-subcarrier intensity modulation performance in strong oceanic turbulence," *Opt. Eng.* **58**(05), 056105 (2019).
10. W. C. Cox, "Simulation, Modeling and Design of Underwater Optical Communication Systems," (PhD Thesis, North Carolina University, Raleigh, North Carolina, USA, 2012).
11. M. Niu, J. Cheng, and J. F. Holzman, "Terrestrial coherent free-space optical communication systems," in *Optical Communication*, (InfTech, 2012).
12. I. Roudas, "Coherent Optical Communication Systems," in *WDM Systems and Networks, Modeling, Simulation, Design and Engineering*, N. Antoniadis, G. Ellinas, and I. Roudas, eds. (Springer, 2012).
13. K. Kikuchi, "Fundamentals of Coherent Optical Fiber Communications," *J. Lightwave Technol.* **34**(1), 157–179 (2016).
14. E. Ip, A. P. T. Lau, D. J. F. Barros, and J. M. Kahn, "Coherent detection in optical fiber systems," *Opt. Express* **16**(2), 753–791 (2008).
15. X. Tang, L. Zhang, C. Sun, Z. Chen, H. Wang, R. Jiang, Z. Li, W. Shi, and A. Zhang, "Underwater Wireless Optical Communication Based on DPSK Modulation and Silicon Photomultiplier," *IEEE Access* **8**, 204676–204683 (2020).
16. B. Zhang, C. Malouin, and T. J. Schmidt, "Design of coherent receiver optical front end for unamplified applications," *Opt. Express* **20**(3), 3225–3234 (2012).
17. M. A. Khalighi and M. Uysal, "Survey on Free Space Optical Communication: A Communication Theory Perspective," *IEEE Commun. Surv. Tutorials* **16**(4), 2231–2258 (2014).
18. R. Hui, "Chapter 9 - Coherent optical communication systems," in *Introduction to Fiber-Optic Communications* (Academic Press, 2020).
19. M. J. Connelly, "COHERENT LIGHTWAVE SYSTEMS," in *Encyclopedia of Modern Optics*, R. D. Guenther, Ed. (Elsevier, 2005).
20. X. Sun, M. Kong, O. Alkhazragi, C. Shen, E.-N. Ooi, X. Zhang, U. Buttner, T. K. Ng, and B. S. Ooi, "Non-line-of-sight methodology for high-speed wireless optical communication in highly turbid water," *Opt. Commun.* **461**, 125264 (2020).
21. A. Laux, R. Billmers, L. Mullen, B. Concannon, J. Davis, J. Prentice, and V. Contarino, "The a, b, c, s of oceanographic lidar predictions: a significant step toward closing the loop between theory and experiment," *J. Mod. Opt.* **49**(3-4), 439–451 (2002).
22. J. Zhao, Y. Liu, and T. Xu, "Advanced DSP for Coherent Optical Fiber Communication," *Appl. Sci.* **9**(19), 4192 (2019).
23. S. Tsukamoto, K. Katoh, and K. Kikuchi, "Coherent demodulation of optical multilevel phase-shift-keying signals using homodyne detection and digital signal processing," *IEEE Photonics Technol. Lett.* **18**(10), 1131–1133 (2006).
24. X. Zhou and J. Yu, "Digital signal processing for coherent optical communication," in *2009 18th Annual Wireless and Optical Communications Conference*, (IEEE, 2009), pp. 1–5.
25. S. J. A. G. Cosijns and M. J. Jansen, "9 - Advanced optical incremental sensors: encoders and interferometers," in *Smart Sensors and Mems*, S. Nihtianov and A. Luque, Eds. (Woodhead Publishing, 2014).
26. A. Marie and R. Alléaume, "Self-coherent phase reference sharing for continuous-variable quantum key distribution," *Phys. Rev. A* **95**(1), 012316 (2017).
27. X. Tang, R. Kumar, S. Ren, A. Wonfor, R. V. Pentyl, and I. H. White, "Performance of continuous variable quantum key distribution system at different detector bandwidth," *Opt. Commun.* **471**, 126034 (2020).
28. T. Pfau, S. Hoffmann, and R. Noe, "Hardware-Efficient Coherent Digital Receiver Concept With Feedforward Carrier Recovery for M-QAM Constellations," *J. Lightwave Technol.* **27**(8), 989–999 (2009).
29. L. Zhang, X. Tang, C. Sun, Z. Chen, Z. Li, H. Wang, R. Jiang, W. Shi, and A. Zhang, "Over 10 attenuation length gigabits per second underwater wireless optical communication using a silicon photomultiplier (SiPM) based receiver," *Opt. Express* **28**(17), 24968–24980 (2020).
30. C. Shen, Y. Guo, H. M. Oubei, T. K. Ng, G. Liu, K.-H. Park, K.-T. Ho, M.-S. Alouini, and B. S. Ooi, "20-meter underwater wireless optical communication link with 1.5 Gbps data rate," *Opt. Express* **24**(22), 25502–25509 (2016).
31. X. Liu, S. Yi, X. Zhou, Z. Fang, Z.-J. Qiu, L. Hu, C. Cong, L. Zheng, R. Liu, and P. Tian, "34.5 m underwater optical wireless communication with 2.70 Gbps data rate based on a green laser diode with NRZ-OOK modulation," *Opt. Express* **25**(22), 27937–27947 (2017).
32. Y. Huang, C. Tsai, Y. Chi, D. Huang, and G. Lin, "Filtered multicarrier OFDM encoding on blue laser diode for 14.8-Gbps seawater transmission," *J. Lightwave Technol.* **36**(9), 1739–1745 (2018).
33. J. Du, Y. Wang, C. Fei, R. Chen, G. Zhang, X. Hong, and S. He, "Experimental demonstration of 50-m/5-Gbps underwater optical wireless communication with low-complexity chaotic encryption," *Opt. Express* **29**(2), 783–796 (2021).

34. C. Lu, J. Wang, S. Li, and Z. Xu, "60 m/2.5Gbps underwater optical wireless communication with NRZ-OOK modulation and digital nonlinear equalization," in *Proc. of Conference on Lasers and Electro-Optics (CLEO)*, (2019).
35. W. Lyu, M. Zhao, X. Chen, X. Yang, Y. Qiu, Z. Tong, and J. Xu, "Experimental demonstration of an underwater wireless optical communication employing spread spectrum technology," *Opt. Express* **28**(7), 10027–10038 (2020).
36. M. Zhao, X. Li, X. Chen, Z. Tong, W. Lyu, Z. Zhang, and J. Xu, "Long-reach underwater wireless optical communication with relaxed link alignment enabled by optical combination and arrayed sensitive receivers," *Opt. Express* **28**(23), 34450–34460 (2020).
37. C. Gabriel, M. Khalighi, S. Bourennane, P. Léon, and V. Rigaud, "Monte-Carlo-Based Channel Characterization for Underwater Optical Communication Systems," *J. Opt. Commun. Netw.* **5**(1), 1–12 (2013).